Bioactive Glass Synthesized by the Acid-free Hydrothermal Method

Ta Anh Tuan
Kazan National Research Technical University named after A N Tupolev: Kazanskij nacional'nyj issledovatel'skij tehniceskij universitet imeni A N Tupoleva-KAI

Elena V. Guseva
Kazan National Research Technical University named after A N Tupolev: Kazanskij nacional'nyj issledovatel'skij tehniceskij universitet imeni A N Tupoleva-KAI

Nguyen Anh Tien
Ho Chi Minh City University of Education

Nguyen Viet Long
Gonzaga University

Le Hong Phuc
Vietnam Academy of Science and Technology

Nguyen Quan Hien
Vietnamese Academy of Science: Vietnam Academy of Science and Technology

Dang Tan Hiep
Ho Chi Minh City University of Food Industry

Vo Thuy Vi
Ho Chi Minh City University of Food Industry

Bui Thi Hoa
Dai Hoc Duy Tan

Bui Manh Ha
Sai Gon University

Bui Xuan Vuongi (buixuanvuongsgu@gmail.com)
Faculty of Pedagogy in Natural Sciences, Sai Gon University, Ho Chi Minh City, 700000, Vietnam
https://orcid.org/0000-0002-3757-1099

Research Article

Keywords: Bioactive glass, acid-free hydrothermal, bioactivity, hydroxyapatite, cell viability

Posted Date: January 13th, 2021

DOI: https://doi.org/10.21203/rs.3.rs-143547/v1

Abstract

Ternary bioactive glass $58SiO_2$-$33CaO$-$9P_2O_5$ (wt.%) was elaborated by the acid-free hydrothermal method. Thermal behavior, textural property, phase composition, morphology, and ionic exchange were investigated by thermal analysis, N_2 adsorption/desorption, XRD, FTIR, SEM, and ICP-OES analysis. The bioactivity and biocompatibility of synthetic bioactive glass were evaluated by in vitro experiments with SBF solution and cell culture medium. The obtained results confirmed that the acid-free hydrothermal process is one of the standard methods for preparing bioactive glass.

Introduction

Bioactive glasses (BGs) have been applied as bone fillers within the clinic for the past fifty years owing to their osteoconductivity and osteoinductivity [1]. These materials possess a special ability to attach with the bone tissue through the formation of a mineral hydroxyapatite layer when soaked in a biological solution. Thereby, broken and defective bones are repaired and filled [2]. Since the primary discovery of bioactive glass ($45SiO_2$-$24.5CaO$-$24.5Na_2O$-$6P_2O_5$, wt.%; commercial name as Bioglass or Novamin), many glass systems have been studied and synthesized using two main methods: melting and sol-gel [3-4]. In particular, the sol-gel method shows outstanding advantages compared to the melting method. The sol-gel processes are often applied to fabricate bioactive glasses at lower temperatures, preventing the loss of the ultimate product due to the evaporation of P_2O_5. Especially, this method can synthesize bioactive glasses on nano-scale with a high value of the specific surface area and porous structures which improve the bioactivity of synthetic materials [5-6]. Nevertheless, most sol-gel processes have used harmful strong acids and bases as catalysts for the hydrolysis of precursors [7-18]. Recently, some scientists have reported on the synthesis of bioactive glasses by the green chemical process. Following this trend, new synthesis processes are being established to cut back or eliminate the utilization or generation of harmful substances [19-20]. A quaternary bioactive glass $75\%SiO_2$-$16\%CaO$-$5\%Na_2O$-$4\%P_2O_5$ (mol.%) has been synthesized by the acid-free sol-gel process [21]. The authors rapidly added the precursors TEOS and TEP in an exceedingly large volume of water, under strong stirring of 1100 rpm. Thereby, the alkoxides hydrolyzed completely to create a transparent sol after 5 h. In our previous study, a binary bioactive glass 70Si-30Ca (mol.%) was made by the acid-free hydrothermal process [22]. A mixture of suitable precursors without catalytic acids was heated in a Teflon lined stainless-steel autoclave at 150 ^oC in an electric oven and kept for 1 day. The resulting product in gel form was dried, and heat-treated at 700 ^oC for 3 hours. The obtained glass was amorphous material and showed interesting bioactivity. Based on this reported paper, we changed some experimental conditions like heated temperature and water/TEOS molar ratio, we emphasize that the acid-free hydrothermal process can be completely applied for synthesizing ternary bioactive glass $58SiO_2$-$33CaO$-$9P_2O_5$ (wt.%). The synthetic glass was characterized, examined for its bioactivity and biocompatibility.

Materials And Methods

2.1. Acid-free hydrothermal synthesis

The acid-free hydrothermal process was used to prepare the bioactive glass $58SiO_2$-$33CaO$-$9P_2O_5$ (wt.%). The composition of the glass system was selected as in previous studies, where the material system was synthesized by the sol-gel method [14-17]. A brief description, a mixture containing 10.42 g of TEOS (Tetraethyl orthosilicate, Sigma-Aldrich, ≥99.0%, Pcode: 102068011), 1.21 g of TEP (Triethyl phosphate, Merck, 100%, CAS-No:78-40-0), 7.09 g of $Ca(NO_3)_2.4H_2O$ (Calcium nitrate tetrahydrate, Merck, 100%, CAS-No-13477-34-4), and 54 g of H_2O was stirred for half-hour. The H_2O/TEOS molar ratio was surveyed and selected at 60. After being mixed together, the mixture was placed in a stainless-steel autoclave lined with Teflon core. The hydrothermal synthesis reactor was programed at 160 ^oC for 24 hours. The gel-producing product was dried at 100 ^oC for 24 hours. From the thermal analysis data, the bioactive glass was obtained by sintering dried powder at 750 ^oC for 3 hours.

2.2. In vitro experiment in SBF fluid

The in vitro test is critical to confirm the bioactivity of synthetic biomaterials before in vivo tests in the animal body. The in vitro test was proposed by Kokubo and Takadama through immersion of the material in the simulated body fluid (SBF) and widely applied for bioactivity evaluation [23]. The SBF synthetic solution has the concentrations of inorganic ions almost similar to the blood of the human body (Tab. 1). It was synthesized by dissolving the appropriate chemical agents comprising of $MgCl_2.6H_2O$, $CaCl_2$, $K_2HPO_4.3H_2O$, $NaHCO_3$, KCl, NaCl, and $C_4H_{11}NO_3$ in distilled water at body temperature of 37 ^oC and pH of 7.4. The powdered glasses were immersed in the SBF solution at 37 ^oC for 1, 3, and 5 days with a stirring speed maintained at 60 rpm. At the end of each soaking stage, the powdered samples were refined, dried, and used for chemical-physical characterization. The remaining solutions were used for ionic measurements.

Table 1. Ionic concentration of SBF solution (mmol/L)

Composition	Na^+	K^+	Ca^{2+}	Mg^{2+}	Cl^-	HCO_3^-	HPO_4^{2-}
SBF	142.0	5.0	2.5	1.5	148.0	4.2	1.0
Plasma	142.0	5.0	2.5	1.5	103.0	27.0	1.0

2.3. In vitro assay within the cellular medium

The cell culture medium was DMEM (Dulbecco's Modified Eagle's Medium, Merck, Product Code D9785) containing 10% FBS, 100 $\mu g.mL^{-1}$ penicillin, 10 $\mu g.mL^{-1}$ streptomycin, and 15 mM HEPES. The L-929

fibroblast line was cultured in DMEM at a temperature of 37 ^{o}C in a humid incubator (5% CO_2, 95% humidity) for 24 hours. The ratio of glass powder/medium was selected as 0.1 g.mL^{-1} according to the ISO standard 10993-12:2004. The various dilutions were obtained from the extract of cellular medium, named as 20%, 40%, 60%, and 100% (without dilution). The fibroblast cells were exposed the extracts for 24 hours. The cellular viabilities on bioactive glass were evaluated by the MTT method consistent with the previous study [24].

2.4. Characterization

The thermal behavior of as-sintering bioactive glass was obtained by employing a Thermogravimetry-Differential Scanning Calorimetry (TG-DSC, Labsys Evo Setaram). The glass powder was put in a platinum crucible, and then heated up from 30 to 1000 ^{o}C in dried air. The textural properties were obtained by using N_2 adsorption/desorption on a micromeritics porosimeter (Quantachrome Instruments). The specific surface area was achieved by using the Brunauer-Emmett-Teller (BET) technique. The pore size and pore volume were calculated from the isotherm desorption curve based on the Barrett-Joyner-Halanda (BJH) method. The phase characteristics of powder samples were identified by X-ray diffraction (XRD, D8-Advance) with Cu-K_{α} radiation (λ = 1.5406Å). The measurements were performed within the range of 5-80° (2θ) with a step of 0.02°. The chemical bonding groups were determined by a Fourier Transferred Infrared Spectroscopy (FTIR, Bruker Equinox 55). The spectral scan was carried out in the range of 400-4000 cm^{-1} with a resolution of 2 cm^{-1}. The Scanning Electron Microscopy (SEM) combined with Energy Dispersive X-rays Spectroscopy (EDX) was employed to identify the morphology and elemental composition of powder samples (SEM, S-4800, Japan). The ionic exchange in SBF solution during in vitro experiment was verified by using an Inductively coupled plasma optical emission spectrometry (ICP-OES, ICP 2060).

Results And Discussion

3.1. Thermal behavior

The thermogravimetry (TG) and the differential scanning calorimetry (DSC) curves of the dried sample are presented in Fig. 1. The TG curve shows three mass-losses at the temperature ranges of 28-210, 210-405, and 405-670 ^{o}C. The primary mass-loss corresponding to the endothermic peak at 123.2 ^{o}C on the DSC curve, assigned to the physically adsorbed-water removal [25]. The second one with an exothermic peak at 298.4 ^{o}C on the DSC curve, is characteristic of the chemically adsorbed-water release [26]. The last one with an endothermic peak centered at 525.3 ^{o}C on the DSC branch, is due to the thermal decomposition of NO_3^- groups used as oxide precursors [27-28]. From temperatures above 670 ^{o}C, no mass-loss is observed. Therefore, the sintering temperature for bioactive glass synthesis is chosen at 750 ^{o}C to eliminate impurities within the sample.

3.2. Textural analysis

The N_2 adsorption/desorption isotherm and pore size distribution of bioactive glass powder are shown in Fig.2. The synthetic bioactive glass exhibits the type IV isotherm, which is suitable for mesoporous material based on the IUPAC classification [29]. The BJH pore size distribution achieved from the desorption branch shows a relatively wide range and a single type distribution with the pore sizes from 8 to 90 nm, concentrated at the mean diameter (MD) of 21.2 nm. The measured values of specific surface area (SSA) and pore volume (PV) are 104.7 m^2/g and 0.54 cm^3/g, respectively. In this study, the synthetic bioactive glass presents interesting values of SSA, PV, and MD compared to the previous reported papers, as shown in Table 2 [15-17].

Tab. 2. Textural properties of synthetic bioactive glass

Reference	Specific Surface Area (m^2/g)	Pore Volume (cm^3/g)	Mean Diameter (nm)	Synthetic Method
[15]	82	0.201	10	Sol-Gel
[16]	99.1	-	-	Sol-Gel
[17]	126.54	0.447	6.55	Sol-Gel
[This Study]	104.7	0.54	21.2	Hydrothermal

3.3. Bioactivity evaluation

3.3.1. XRD analysis

Fig. 3 shows the XRD diagrams of glass samples before and after in vitro experiments in the SBF solution. The XRD pattern of synthetic bioactive glass exhibits a wide diffraction halo centered at about 23^o (2θ). This is a typical characteristic of an amorphous material, confirming the successful synthesis of ternary bioactive glass $58SiO_2$-$33CaO$-$9P_2O_5$ (wt.%) by the free-acid hydrothermal method. After the primary day in SBF solution, the bioactive glass showed two well-defined peaks at $2\theta=26^o$ (002) and 32^o (211), which are attributed to crystalline hydroxyapatite (HA) phase (well matched with JCPDS card number 90432). As increasing the soaking time, these two peaks became sharper and higher in intensity. After 5 days, most of the representative peaks of the HA phase have appeared clearly, demonstrating the bioactivity of synthetic bioactive glass in this study.

3.3.2. FTIR analysis

Fig. 4 represents the FTIR spectra of bioactive glass before and after in vitro experiment in SBF fluid. The spectrum of synthetic glass represents the most characteristic bands of the silica network. The band at

1104 cm^{-1} is attributed to the Si-O-Si asymmetric stretching vibration (asym) while the band at 803 cm^{-1} corresponds to the Si-O-Si symmetric stretching vibration (sym) [30]. The band observed at 470 cm^{-1} is characteristic of Si-O-Si bending vibration [31]. The weak band at 977 cm^{-1} is ascribed to the Si-O non-bridging oxygen (NBO) stretching mode [30]. Only a weak band at 554 cm^{-1} related to the stretching mode of PO_4^{3-} [32-33], is observed because of the low content of P_2O_5 in synthetic bioactive glass. After in vitro experiment in SBF for 1, 3 and 5 days, the spectral feature of glass is modified, thanks to the chemical interactions between the glass samples and the physiological medium. The spectral band at 1104 cm^{-1} (Si-O-Si asym) is shifted to 1030 cm^{-1}. The band at 803 cm^{-1} (Si-O-Si sym) is moved to 869 cm^{-1}. The band at 470 cm^{-1} (Si-O-Si ben) is displaced to 460 cm^{-1}. The band at 977 cm^{-1} (Si-O-NBO) is disappeared. The Si-O-Si shift and Si-O disappearance are associated with the glassy-network dissolution, and then the re-polymerization of -$Si(OH)_4$ groups to make the SiO_2 rich surface layer [30-33]. Typically, two well-defined bands at 564 and 600 cm^{-1} are revealed. They are attributed to the stretching modes of PO_4^{3-} groups in the hydroxyapatite crystals [34-35]. The FTIR result associated with the XRD analysis emphasize the bioactivity of bioactive glass synthesized by the free-acid hydrothermal method.

3.3.3. SEM-EDX analysis

Fig.5 shows the SEM micrographs including EDX analyses of the glass samples before and after immersion in SBF fluid for 5 days. The SEM image of synthetic glass shows agglomerates consisting of intertwined tiny particles, forming the three-dimensional mesoporous structure of synthetic material. The EDX analysis gives the Si/Ca/P molar ratio of 7.52/4.41/1, which is quite similar to the theoretical ratio in synthetic glass ($60SiO_2$-$36CaO$-$4P_2O_5$ mol.%; Si/Ca/P = 7.5/4.5/1). After 5 days of immersion in the SBF solution, the surface of the bioactive glass is replaced and completely recovered by a uniform, scaled crystal layer. The EDX analysis of glass after 5 days in SBF shows a decrease in Si content because of the degradation of glassy network, and a rise in Ca, P amounts due to the formation of HA phase. The calculated Ca/P molar ratio for 5 days is 1.72, similar to that of pure apatite [26-27]. The SEM observation and EDX analysis confirm the appearance of a new apatite layer on the surface of bioactive glass.

3.3.3. ICP-OES analysis

Physical-chemical interactions of bioactive glass with the physiological environment lead to ionic changes in the SBF solution. Elemental concentrations of Si, Ca, P in the initial SBF solution were 0 ppm, 100.2 ppm, and 31.4 ppm, respectively. The Si concentration rapidly increased at the beginning time of soaking, and then moderately increased after 3 days. The concentration of Si recorded the saturation after 5 days of immersion. According to the previous studies, a rising in Si concentration is explained by the dissolution of the glassy network through the release of silicic acid $Si(OH)_4$ while the saturation process corresponds to the re-polymerization of the above acids to create SiO_2 silica layer [30-33]. On the other hand, the concentration of Ca increases at the beginning time of soaking, probably due to the quick exchange of Ca^{2+} out of the glassy network and H^+ in the physiological fluid [34-36]. Thereafter, the

concentration of Ca strongly decreased after 3 days and reach to the saturation at 5 days. The decrease of Ca concentration is expounded by its consumption to make the mineral HA layer on the surface of bioactive glass [34-36]. By contrast, no increase in P concentration was observed after in vitro experiment. This can be explained by the low content of P_2O_5 in the synthetic glass and also the rapid consumption of Ca, and P for the formation of the apatite mineral layer. This result completely fits with XRD analysis where the HA layer was determined after just 1 day of soaking in the SBF solution.

3.4. Biocompatibility evaluation

The cell viabilities of L-929 fibroblast cells directly contact with bioactive glass powder for 24 hours are presented in Fig. 7. The cell viability without contact in bioactive glass was selected as the control (100%) [24]. The obtained results show that the cell viabilities were 124, 116, 96, 94% for 20%, 40%, 60%, and 100% extracts, respectively. Therefore, the 20% extract showed the highest value of cell viability while 60% and 100% extracts present small difference. Following the standard ISO 10993-5 (Biological evaluation of medical devices – Part 5: Test for cytotoxicity, in vitro methods 2009), the cell viability is calculated as a percentage relative to the control, set as 100%. In the case where the average of cell viability is less than 70%, the material is cytotoxic. Therefore, the bioactive glass $58SiO_2$-33CaO-$9P_2O_5$ (wt.%) synthesized by the acid-free hydrothermal method presented the good biocompatibility in the cellular medium even within the high extracts.

Conclusion

This study confirmed that the acid-free hydrothermal method is suitable for the synthesis of ternary bioactive glass $58SiO_2$-33CaO-$9P_2O_5$ (wt.%). The obtained bioactive glass has amorphous and mesoporous structures. The bioactivity of synthetic glass was proved through the rapid formation of the hydroxyapatite mineral layer on the surface of glass samples after in vitro experiment in SBF fluid. In addition, the in vitro experiment in the cellular environment demonstrated the good biocompatibility of synthetic bioactive glass.

References

[1] M.N. Rahaman, D.E. Day, B.S. Bal, Q. Fu, S.B. Jung, L.F. Bonewald, A.P. Tomsia, Acta. Biomater. 7 (2011) 2355–2373.

[2] L.L. Hench, J. Mater. Sci. Mater. Med. 17 (2006) 967–978.

[3] R.J. Julian, Acta. Biomater. 9 (2013) 4457– 4486.

[4] F. Baino, et al, J. Non. Cryst. Solids. 432 (2016), 15–30.

[5] A.R Boccaccini, M. Erol, W. Stark, Compos. Sci. Technol. 70 (13) (2010) 1764–1776.

[6] K. Zheng, A.R. Boccaccini, Adv. Coll. Interf. Sci.249 (2017) 363–373.

[7] F. Sharifianjazi, N. Parvin, M. Tahriri, J. Non. Cryst. Solids. 476, (2017) 108–113.

[8] A. Vulpoi, et al, Mater. Sci. Eng. C 32 (2012) 178–183.

[9] A. Balamurugan, et al, Acta. Biomater, 3 (2) (2007), 255–262.

[10] S. Salman, S. Salama, H. Abo-Mosallam, Ceram. Int. 38 (2012) 55–63.

[11] A. El-Kheshen, et al, Ceram. Int. 34 (7) (2008) 1667–1673.

[12] F. Baino, et al, Mater. Lett. 235, (2019) 207–211

[13] A. Bari, et al, Acta. Biomater.55 (2017), 493–504.

[14] M. Bini, S. Grandi, D. Capsoni, P. Mustarelli, E. Saino, L. Visai, J. Phys. Chem. C. 113 (2009) 8821–8828.

[15] J. Bejarano1, P. Caviedes, H. Palzal, Biomed. Mater. 10 (2015) 1–13.

[16] X.V. Bui, T.H. Dang, Process. App. Ceram. 13 (1) (2019) 98–103.

[17] P. Sepulveda, J.R. Jones, L.L. Hench, J. Biomed. Mater. Res. 58 (6) (2001) 734–740.

[18] A. Balamurugan, G. Balossier, S. Kannan, J. Michel, A.H.S. Rebelo, J.M.F. Ferreira, Acta. Biomater. 3 (2007) 255–262.

[19] R.A. Sheldon, I.W.C.E. Arends, U. Hanefeld, Green Chemistry and Catalysis, Wiley VCH, 2007.

[20] J.H. Clark, D.J. Macquarrie, Green Chemistry and Technology, Abingdon (2008)

[21] B.A.E. Ben-Arfa, H.R. Fernandes, I.M.M. Salvado, J.M.F. Ferreira, R.C. Pullar, J. Am. Ceram. Soc. 101 (7) (2018) 2831–2839.

[22] B.T. Hoa, H.T.T. Hoa, N.A. Tien, N.H.D. Khang, E.V. Guseva, T.A. Tuan, B.X. Vuong, Mater. Lett. 274 (2020) 1–4.

[23] T. Kokubo, H. Takadama, Biomater. 27 (15) (2006) 2907–2915.

[24] T. Mosmann, J. Immunol. Meth. 65 (1983) 55–63.

[25] A. Saboori, M. Rabiee, F. Moztarzadeh, M. Sheikhi, M. Tahriri, M. Karimi, Mater. Sci. Eng. C. 29 (1) (2009) 335–340.

[26] A.M. El-Kady, A.F. Ali, Ceram. Int. 38 (2012) 1195–1204.

[27] J.R.J. Delben, K. Pereira, S.L. Oliveira, L.D.S. Alencar, A.C. Hernandes, A.A.S.T. Delben, J. Non-Cryst. Solids. 361 (2013) 119–123.

[28] J. Román, S. Padilla, M. Vallet-Regí, Chem. Mater. 15 (2003) 798–806.

[29] M. Thommes, K. Kaneko, A.V. Neimark, J.P. Olivier, F. Rodriguez-Reinoso, J. Rouquerol, K.S.W. Sing, Pure. Appl. Chem. 87 (9,10) (2015) 1–19.

[30] V. Aina, G. Malavasi, A. Fiorio Pla, L. Munaron, C. Morterra, Acta. Biomater. 5 (2009) 1211–1222.

[31] I.Y. Kim, G. Kawachi, K. Kikuta, S.B. Cho, M. Kamitakahara, C. Ohtsuki, J. Eur. Ceram. Soc. 28 (2008) 1595–1602.

[32]. P. Innocenzi, J.Non-Cryst. Solids, 316 (2003) 309–319.

[33]. J. Ding, Y. Chen, W. Chen, L. Hu, G. Boulon, Chin. Opt. Lett. 10 (7) (2012) 071602.
[34] X.F. Chen, B. Lei, Y.J. Wang, N. Zhao, J. Non-Cryst. Solids. 355 (2009) 791–796.
[35] Z. Hong, A. Liu, L. Chen, X. Chen, X. Jing, J. Non-Cryst. Solids 355 (2009) 368–372.

[36]. A. Hoppe, N.S. Güldal, A.R. Boccaccini, Biomater. 32 (2011) 2757–2774.

Figures

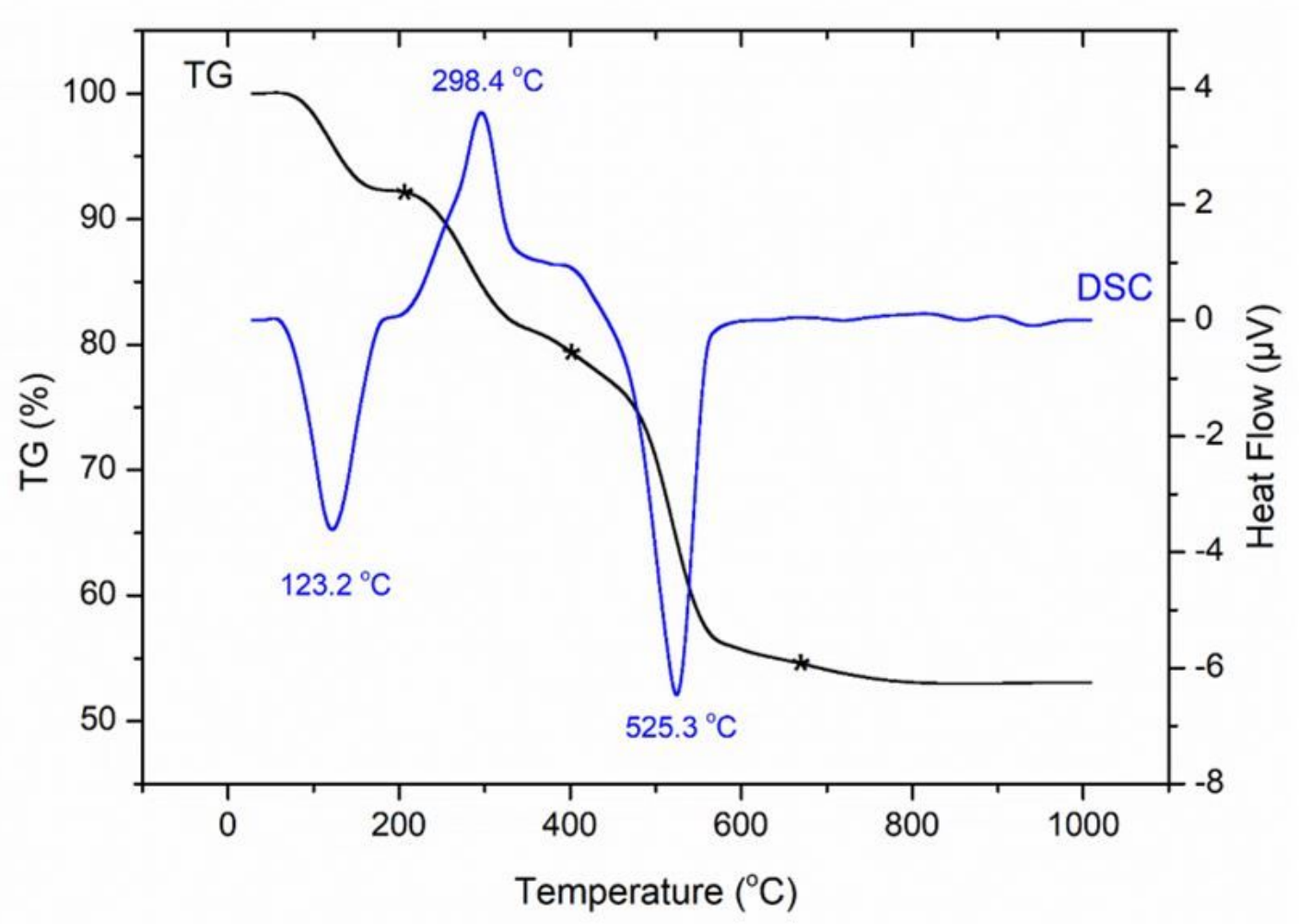

Figure 1

TG-DSC curves of the as-sintering bioactive glass sample

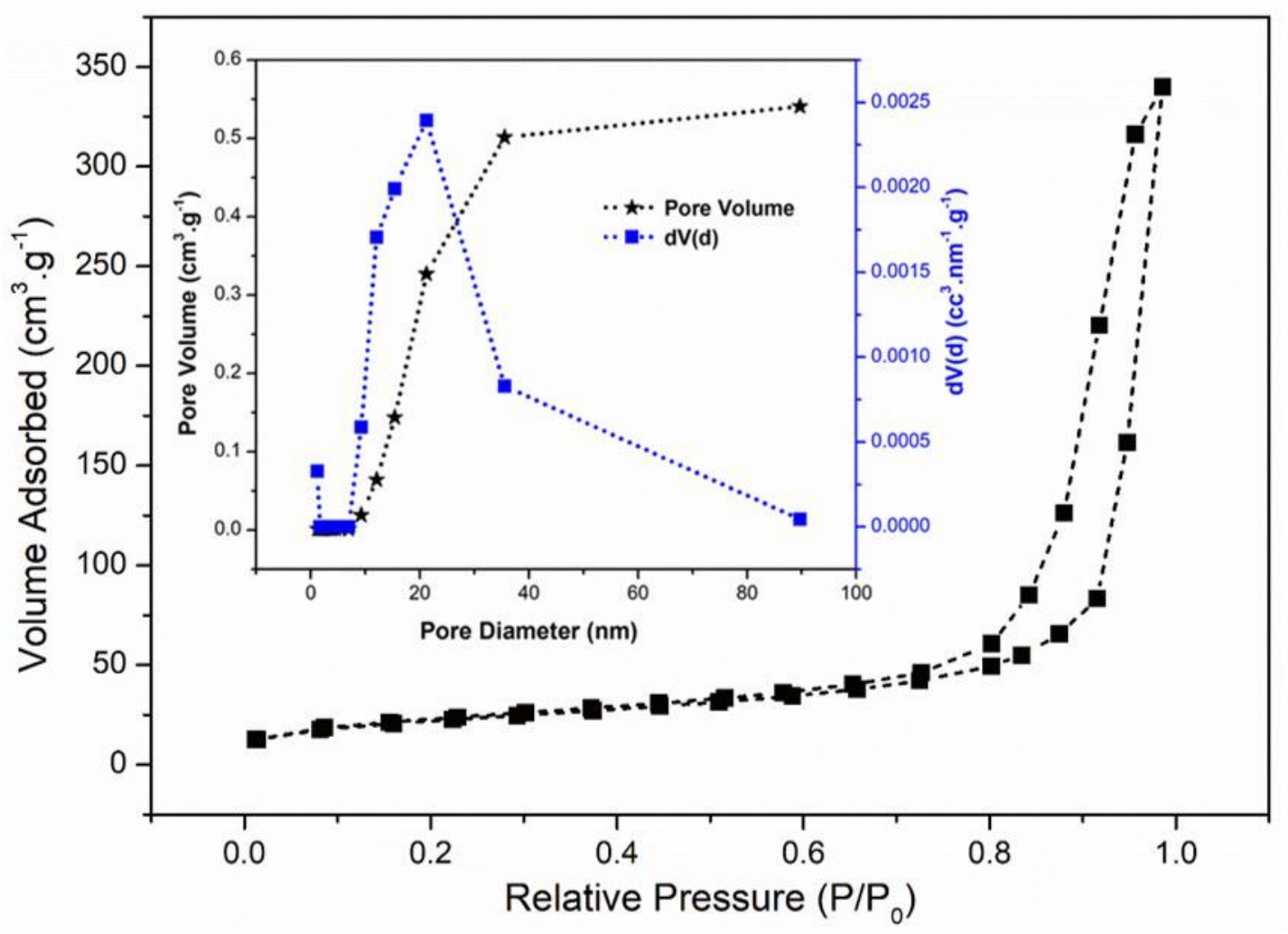

Figure 2

Nitrogen adsorption/desorption isotherm and pore size distribution of bioactive glass

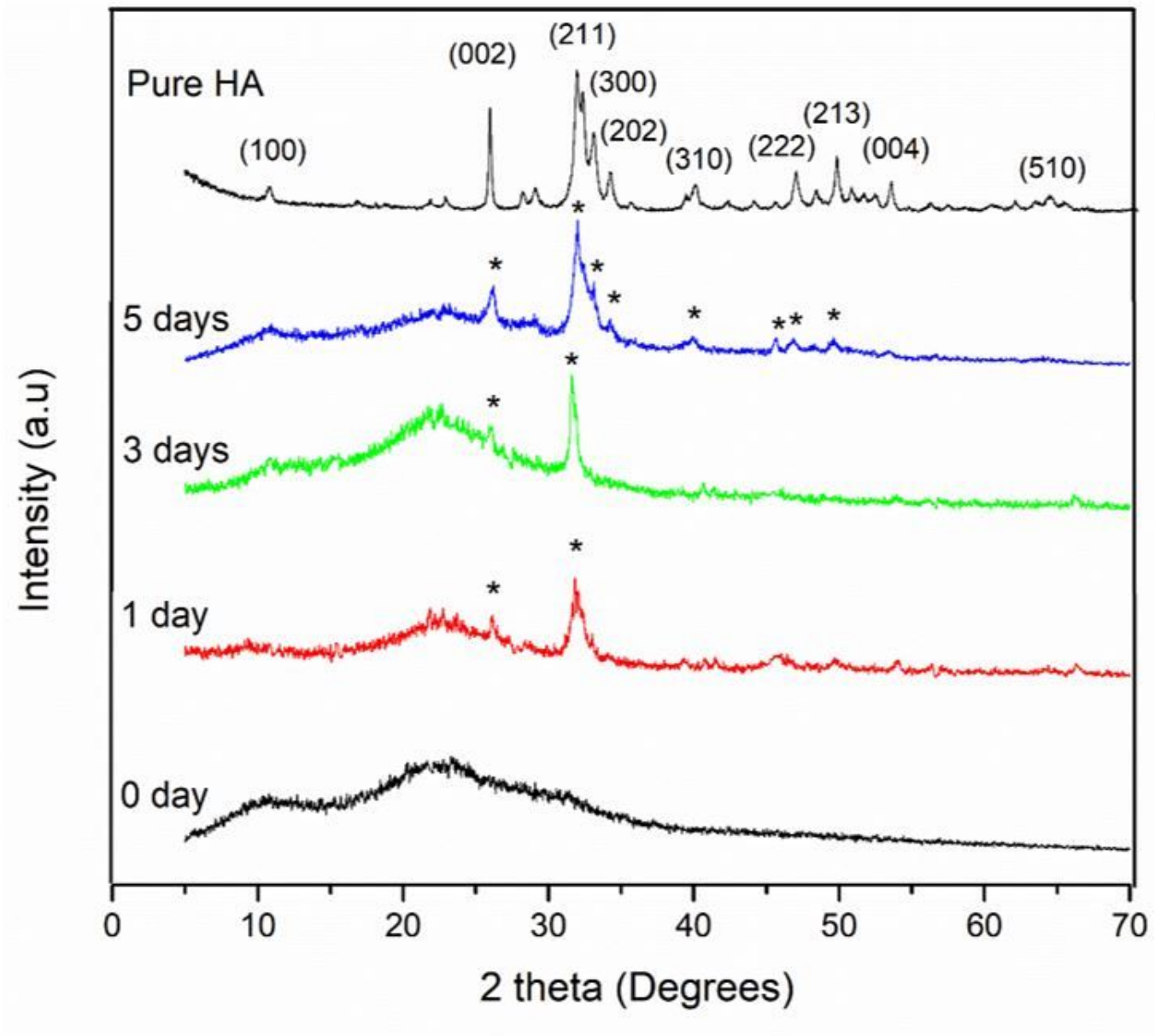

Figure 3

XRD diagrams of bioactive glass before and after in vitro experiment in SBF

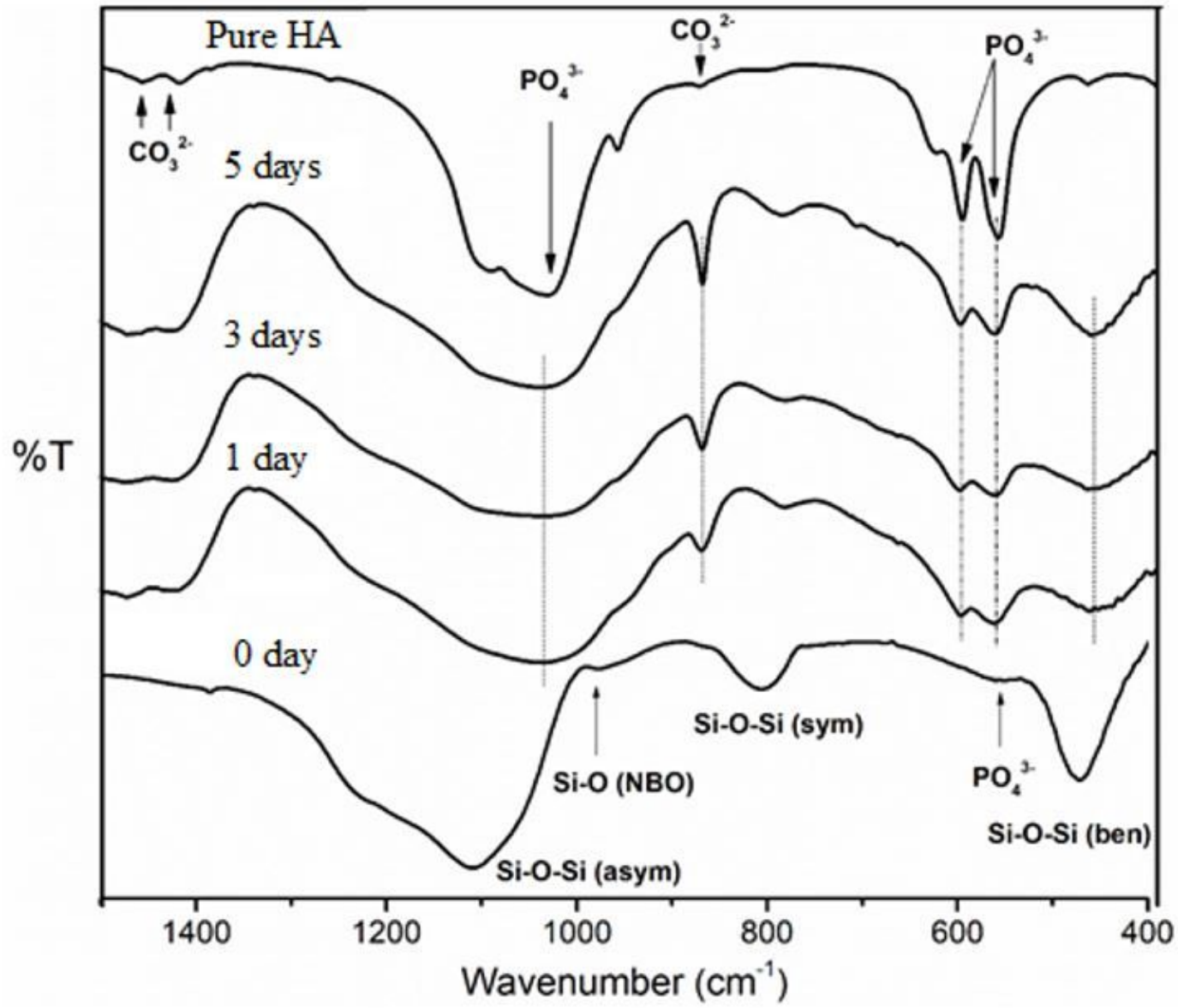

Figure 4

FTIR spectra of bioactive glass before and after in vitro experiment in SBF

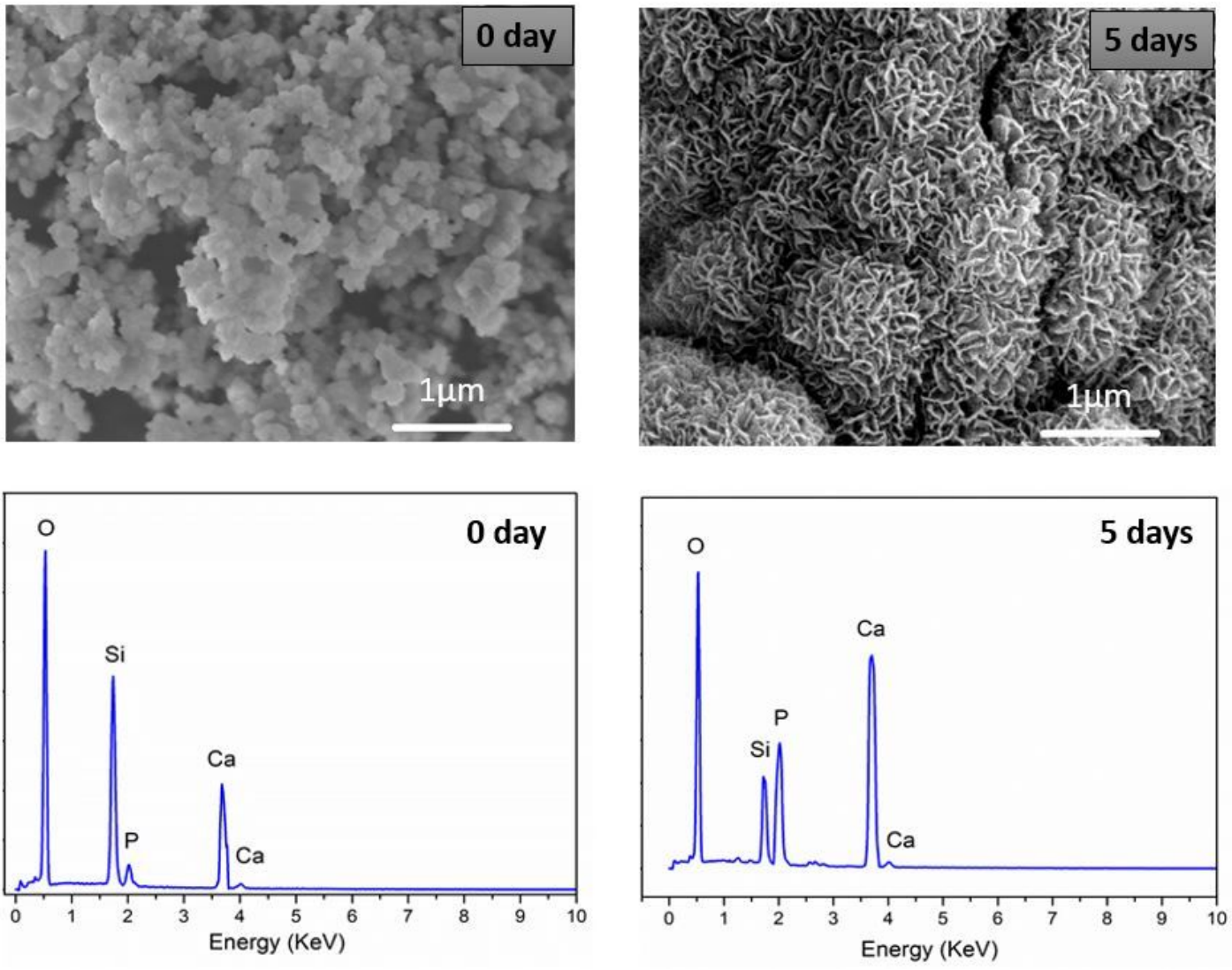

Figure 5

SEM-EDX analyses of bioactive glass before and after 5 days of immersion

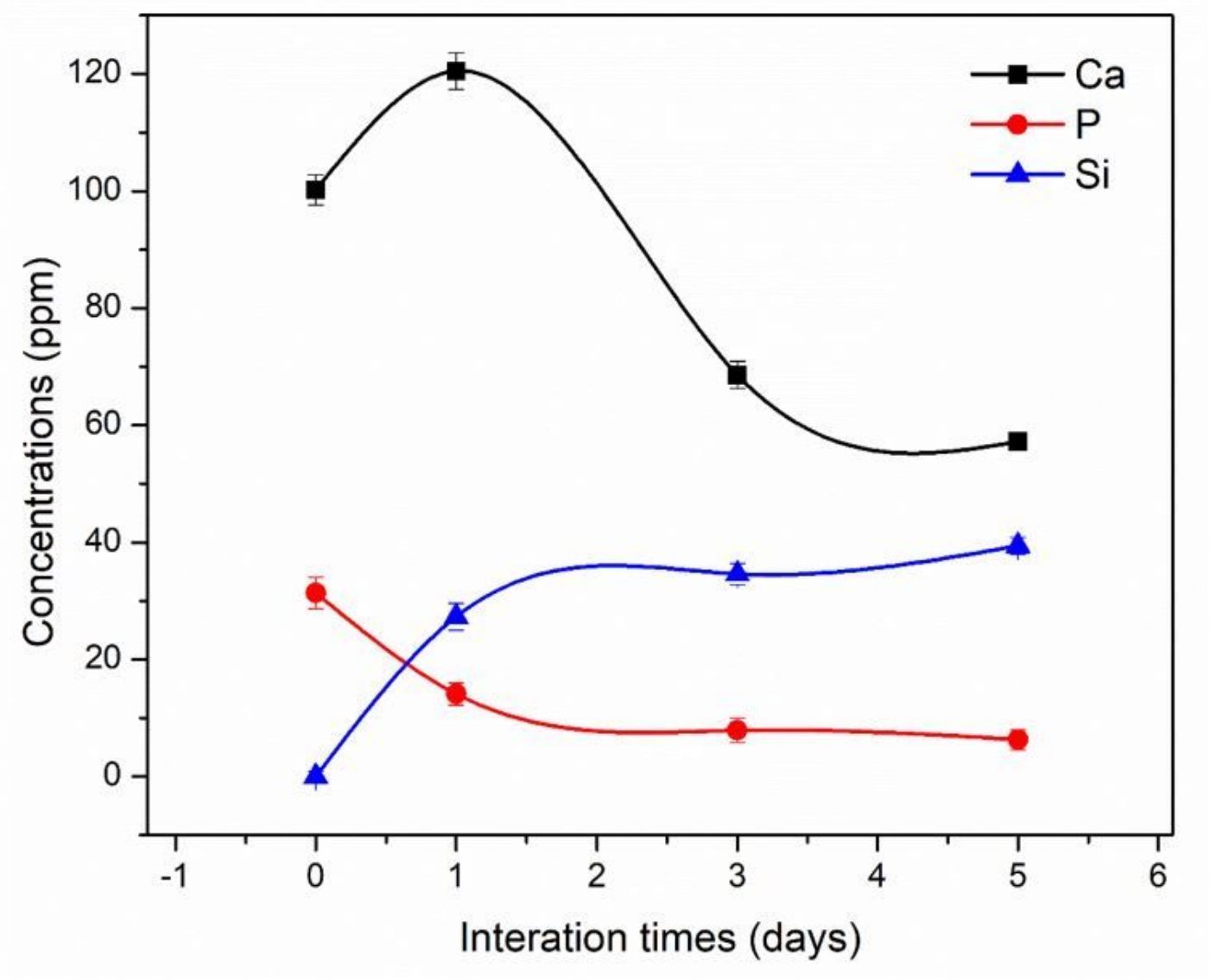

Figure 6

Ionic exchanges between the bioactive glass and the SBF solution

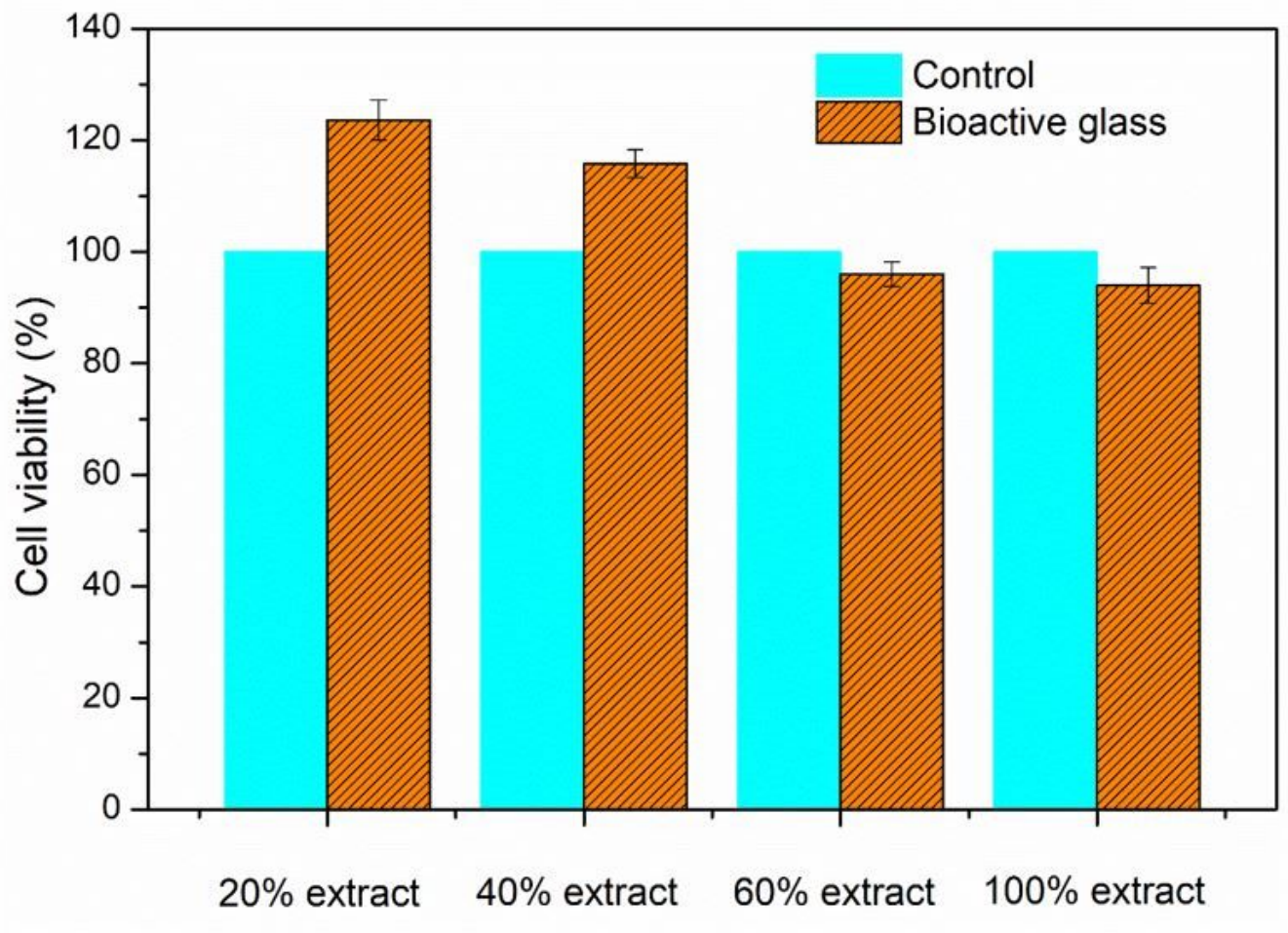

Figure 7

Cell viabilities of synthetic bioactive glass